NASA TECHNICAL MEMORANDUM

NASA TM X- 72813

(NASA-TM-X-72813) ANALYTICAL AND EXPERIMENTAL STUDY OF STRUCTURALLY EFFICIENT COMPOSITE HAT-STIFFENED PANELS LOADED IN AXIAL COMPRESSION (NASA) 23 p HC $3.50 CSCL 20K G3/39

N76-18528

Unclas 14783

NASA TM X- 72813

ANALYTICAL AND EXPERIMENTAL STUDY OF STRUCTURALLY EFFICIENT COMPOSITE HAT-STIFFENED PANELS LOADED IN AXIAL COMPRESSION

By Jerry G. Williams and Martin M. Mikulas, Jr.

January 7, 1976

MAR 1976
RECEIVED
NASA STI FACILITY
INPUT BRANCH

This informal documentation medium is used to provide accelerated or special release of technical information to selected users. The contents may not meet NASA formal editing and publication standards, may be revised, or may be incorporated in another publication.

NATIONAL AERONAUTICS AND SPACE ADMINISTRATION
LANGLEY RESEARCH CENTER, HAMPTON, VIRGINIA 23665

1. Report No.	2. Government Accession No.	3. Recipient's Catalog No.
NASA TM X-72813		

4. Title and Subtitle	5. Report Date
ANALYTICAL AND EXPERIMENTAL STUDY OF STRUCTURALLY EFFICIENT COMPOSITE HAT-STIFFENED PANELS LOADED IN AXIAL COMPRESSION	JANUARY 1976
	6. Performing Organization Code
7. Author(s)	8. Performing Organization Report No.
Jerry G. Williams and Martin M. Mikulas, Jr.	
	10. Work Unit No.
9. Performing Organization Name and Address	
NASA Langley Research Center Hampton, Va. 23665	11. Contract or Grant No.
	13. Type of Report and Period Covered
12. Sponsoring Agency Name and Address	Technical Memorandum
National Aeronautics and Space Administration Washington, D. C. 20546	14. Sponsoring Agency Code

15. Supplementary Notes

Paper presented at ASME/AIAA/SAE 16th Structures, Structural Dynamics, and Materials Conference, May 1975, AIAA Paper No. 75-754.

16. Abstract

Structural efficiency studies were made to determine the weight saving potential of graphite/epoxy composite structures for compression panel applications. Minimum weight hat-stiffened and open corrugation configurations were synthesized using a nonlinear mathematical programing technique. Selected configurations were built and tested to study local and Euler buckling characteristics. Test results for 23 panels critical in local buckling and six panels critical in Euler buckling are compared with analytical results obtained using the BUCLASP-2 branched plate buckling program. A weight efficiency comparison is made between composite and aluminum compression panels using metal test data generated by the NACA. Theoretical studies indicate that potential weight savings of up to 50% are possible for composite hat-stiffened panels when compared with similar aluminum designs. Weight savings of 32% to 42% were experimentally achieved. Experience to date suggests that most of the theoretical weight saving potential is available if design deficiencies are eliminated and strict fabrication control is exercised.

17. Key Words (Suggested by Author(s))	18. Distribution Statement
Composite structure Structural efficiency	Unclassified - Unlimited

19. Security Classif. (of this report)	20. Security Classif. (of this page)	21. No. of Pages	22. Price*
Unclassified	Unclassified	21	$3.25

*For sale by the National Technical Information Service, Springfield, Virginia 22161

ANALYTICAL AND EXPERIMENTAL STUDY OF STRUCTURALLY EFFICIENT COMPOSITE HAT-STIFFENED PANELS LOADED IN AXIAL COMPRESSION *

Jerry G. Williams and Martin M. Mikulas, Jr.
NASA Langley Research Center
Hampton, Virginia 23665

Abstract

Structural efficiency studies were made to determine the weight saving potential of graphite/epoxy composite structures for compression panel applications. Minimum weight hat-stiffened and open corrugation configurations were synthesized using a nonlinear mathematical programming technique. Selected configurations were built and tested to study local and Euler buckling characteristics. Test results for 23 panels critical in local buckling and six panels critical in Euler buckling are compared with analytical results obtained using the BUCLASP-2 branched plate buckling program. A weight efficiency comparison is made between composite and aluminum compression panels using metal test data generated by the NACA. Theoretical studies indicate that potential weight savings of up to 50% are possible for composite hat-stiffened panels when compared with similar aluminum designs. Weight savings of 32% to 42% were experimentally achieved. Experience to date suggests that most of the theoretical weight saving potential is available if design deficiencies are eliminated and strict fabrication control is exercised.

Symbols

A	Area
B	Panel width
b_i	Dimension of panel element i
E_1	Lamina modulus in fiber direction
E_2	Lamina modulus transverse to fiber direction
G_{12}	Lamina shear modulus
L	Panel length
L_e	Effective panel length
m	Buckle mode half wave number
N_x	Buckling stress resultant
P_E	Euler buckling load
t_i	Thickness of element i
W	Panel weight
$\bar{\varepsilon}_x$	Critical strain in x-direction
θ	Composite ply orientation angle
ν_{12}	Major Poisson's ratio
ρ	Density

*Paper presented at ASME/AIAA/SAE 16th Structures, Structural Dynamics, and Materials Conference, May 1975, AIAA Paper No. 75-754.

Introduction

Over the past 5 to 10 years a substantial amount of composite material hardware has been developed, however, most of this hardware has been in the form of flight components or demonstration articles. Extraction of fundamental structural data from such special-purpose hardware programs is very difficult if not impossible. Test programs on generic structural components for which structural parameters are systematically varied appear to be completely lacking in the literature. In order to take full advantage of the potential offered by advanced composite materials, data necessary for design are needed on all phases of structural behavior including material strength, skin buckling, overall buckling, and deformation behavior, as well as other characteristics which are peculiar to composite construction.

The information presented herein represents the initial results of a program initiated at the Langley Research Center to establish a weight and strength data base for efficient graphite/epoxy compression panels of stiffened construction. The hat-stiffened configuration was selected for initial comprehensive studies due to its known structural efficiency and the relatively predictable nature of the buckling behavior of closed section stiffeners. Composite material open section stiffeners, such as J and Z configurations are known to exhibit stiffener roll and modal interaction behavior[1] at much lower loads than closed section stiffeners. To date, this behavior has not been characterized by a "classical" closed-form analytical model suitable for inclusion in an automated design program. Since a rapid analysis was important for the purposes of the current design, a comprehensive examination of the open section stiffener geometry has been deferred until a suitable analysis can be efficiently coupled with a design synthesis program. In addition to the hat configuration, limited studies have been made of an open corrugation configuration and results are reported herein.

The general approach taken in the present study is quite different from the approach used by the NACA during the 1940's[2-6] where thousands of aluminum panels with parametrically varied dimensions were tested to develop structural design allowables and efficiency charts. Because of the much larger number of design variables associated with composite materials as compared with aluminum, it was necessary to use automated design methods for the identification of efficient panel cross sections for experimental evaluation. An advanced version of the mathematical programing design method developed in Reference 7 was used for this purpose. Panel designs were constrained to insure fabricability and selected panel designs were chosen for experimental evaluation. For each cross-sectional geometry selected, short specimens were used to evaluate

REPRODUCIBILITY OF THE ORIGINAL PAGE IS POOR

local buckling and ultimate strength, and longer wide-column specimens were used to evaluate Euler and interactive buckling modes. Buckling results are compared with the BUCLASP-2 branched plate buckling analysis program.[8,9] The performance of graphite/epoxy compression panels is presented in the form of structural efficiency charts for ready comparison with other configurations and other material systems.

Panel Design and Analysis

Three panel cross-sectional configurations are considered in the present investigation and are shown schematically in Sketch a. The shaded and unshaded areas distinguish between the orientations of the plies and their distribution. The first cross section, labeled configuration A, was identified in Reference 7 as being a structurally efficient arrangement for carrying axial compression loads with the ply orientation angle θ being $\pm 45°$. The essential features of this design are (1) that 0° (high axial stiffness) plies are located in the hat cap and skin to provide maximum column bending stiffness and (2) that the vertical webs are composed of all $\pm\theta$ (low axial stiffness) plies to minimize the amount of axial load carried by the webs, thus suppressing local buckling. Also, the $\pm\theta$ plies in the vertical webs provide the shearing stiffness needed to minimize column transverse shearing deformations. A second design, which was found to be very efficient, had 0° plies concentrated under the hat. This concept is labeled as configuration B in Sketch a. The third panel cross section considered was a symmetrical open corrugation and is shown in Sketch a as configuration C.

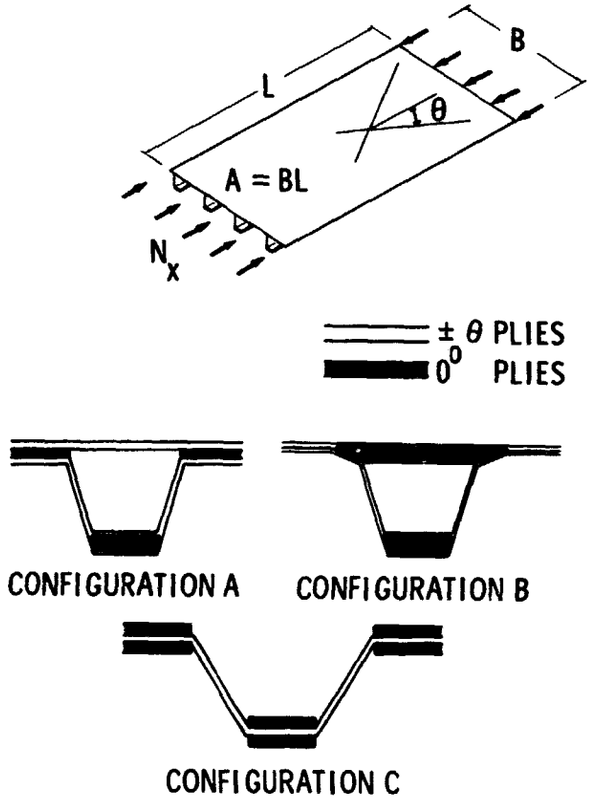

Sketch a — Compression panel configuration options

The panel designs were achieved by formulating the problem in terms of simple analytical relationships and using a nonlinear mathematical programing technique to search for minimum weight geometric proportions. A more sophisticated analysis was used to determine the adequacy of the simplified design analyses to represent correctly the buckling behavior of the panels. Modifications were made in the synthesis code when deficiencies were indicated. Selected panel designs were fabricated and subjected to experimental evaluation. For each design selected, specimens 16 inches long were used to evaluate local buckling and ultimate strength, and specimens 60 inches long were used to evaluate Euler and interactive buckling modes. Test results are reported for 23 16-inch-long specimens, and for six 60-inch-long specimens. Experimental results are compared with BUCLASP-2 analytical results.

Panel Cross-Section Definition

A description of the general panel cross section considered is shown in Figure 1. Nine design variables are used to define the panel cross section, which include four element widths b_i and five thicknesses t_i. The cross section may be considered to be constructed of four basic elements. Element 1 is the skin under the hat, element 2 is the stiffener web, element 3 is the hat cap, and element 4 is the skin between stiffeners. For configuration A of Sketch a, the thickness variable t_5 is taken to be equal to zero. For configuration B, the thickness variable t_4 was taken to be zero and the t_5 material is linearly tapered at the ends and extends 0.35 inch into element 4. For the open corrugated panel, configuration C, the thickness variables t_1 and t_2 are taken to be equal to zero and the t_4 0° material is distributed symmetrically about the $\pm\theta$ material.

Design Method

The design rationale was to seek minimum weight panel proportions subject to the following constraints:

1. The local buckling load of the skin and stiffeners is not to be exceeded.

2. The wide-column Euler buckling load is not to be exceeded.

3. A prescribed allowable axial strain is not to be exceeded.

4. Geometric proportions are to lie within prescribed limits dictated by practical or manufacturing considerations.

A listing of numerical values of the upper and lower bounds placed on the geometric constraints and critical strain in this investigation are presented in Table I. An important difference between the design approach used herein and one commonly used for metal structures is that all panel elements are not required to buckle simultaneously. Instead, buckling of the various elements is introduced as constraints in the design process in which it is only required that individual element buckling loads not be exceeded. Local buckling is never critical in certain elements of the composite panel cross section as is discussed subsequently.

The design calculations were made using an advanced version of the design method developed in Reference 7. This code uses classical closed-form solutions for buckling and a nonlinear mathematical programing technique to search for minimum weight cross-sectional dimensions. Local buckling calculations for each plate element are based on the buckling load for an infinitely long orthotropic plate simply supported along the two unloaded edges. For overall buckling, the panel is assumed to behave as an Euler wide column.

Analysis Methods

For panel designs and comparison with experiments, three different analytical approaches were used for buckling calculations and are listed as follows:

1. Classical Closed-Form Solutions. Provided the rapid buckling calculations required in the synthesis program to achieve a minimum weight design. A detailed description of these analyses is given in Appendix B of Reference 7.

2. BUCLASP-2. An advanced branched plate buckling analysis which was used to evaluate the adequacy of the classical analyses used in the synthesis code and to compare with the experimental results. BUCLASP-2, which is presented in References 8 and 9, treats stiffener rolling and modal interactions but is limited to orthotropic plate elements. Prebuckling deformations are ignored and the loaded edges are simply supported. Boundary conditions at lateral edges are arbitrary and residual thermal strains are ignored.

3. BUCLAP2. An advanced anisotropic plate buckling analysis which was used to investigate anisotropic effects on the local buckling of relatively thin plate elements. A description of BUCLAP2 is presented in Reference 10.

Discussion of Design Program Deficiencies and Refinements

During the course of the present investigation, several important structural phenomena were observed that were not considered in the design synthesis method of Reference 7. Phenomena considerations which were uncovered by the experimental studies or by comparisons with BUCLASP-2 and BUCLAP2 are:

1. Anisotropic effect — This effect is important for a relatively thin four-ply laminate.

2. Column transverse shearing effect — This effect is important for certain combinations of load ranges and vertical web thicknesses.

3. Element local buckling boundary conditions other than simple support — For heavier load ranges, minimum weight panel proportions were such that boundary conditions offering more restraint than simple support were appropriate.

4. Residual thermal strains — Due to the different coefficients of thermal expansion in adjacent plate elements caused by different laminate layups, residual thermal strains were induced during the cool-down phase of the cure cycle.

5. Panel warping — As in item 4, the different coefficients of thermal expansion caused warping of the panel during cooling from the cure temperature which affects the column buckling load.

Anisotropic Effects. To eliminate stretching/bending coupling, all elements were laid up with midplane symmetry. In general, however, a midplane symmetric laminate does possess bending/twisting coupling which reduces the local buckling load for a plate element.[11] Calculations made with BUCLAP2 on long plates simply supported on the unloaded edges indicated that the reduction in the buckling load due to anisotropic effects as compared with the orthotropic value is 24% for a four-ply $(\pm 45/\pm 45)$ graphite/epoxy laminate and 1.2% for an eight-ply $(\pm 45/\overline{\pm 45})_S$ graphite/epoxy laminate. Calculations from BUCLAP2 for the buckling loads and strains of a long four-ply $(\pm\theta/\overline{\pm\theta})$ plate are presented in Figure 2 as a function of θ. Results are given for both the simply supported and clamped cases. The design program used in the present investigation was modified to account for the 24% anisotropic reduction in the local buckling load for four-ply laminates and the anisotropic effect was neglected for thicker laminates.

The weight penalty imposed by including anisotropic effects for elements 1 and 2 of Figure 1 are presented in Figure 3 which shows panel weight per unit area per unit length (W/AL) as a function of the load index (N_x/L). Although a relatively large (24%) load reduction may result from anisotropic effects, it can be seen from Figure 3 that very little loss in structural efficiency results if the effect is included in the design synthesis program.

Transverse Shearing Effects. The expression for inlcuding transverse shearing deformations in the buckling of a column is taken from Reference 12 as

$$P_{cr} = \frac{P_E}{1 + \frac{\beta P_E}{G\bar{A}}}$$

where for these panels $\bar{A}$ is equal to the web cross-sectional area and G is the in-plane shear modulus of the vertical web laminate. Taking these values for $\bar{A}$ and G assumes that all of the shearing deformation occurs in the vertical web (element 2). In the current design program, the above equation was used to account for column transverse shearing with the shape factor β taken as 1. Panel weight minimization studies showed very small weight penalties resulted by imposing this constraint. Ignoring this effect, however, can result in significant reductions in the actual load the panel can carry. For example, a panel designed for a load index N_x/L of 300 lb/in^2 using a 0.022-inch-thick web was shown theoretically to buckle at a load 10% lower than the value predicted when column transverse shearing deformations were ignored.

Element Local Buckling Boundary Conditions. For lightly to moderately loaded panels ($N_x/L < 100$ lb/in^2) minimum weight configurations are characterized by cross-section skin and web elements which have width-to-thickness ratios (b_i/t_i) of the same order

of magnitude. The hat cap width is usually limited by the 0.8-inch minimum gage constraint (Table I) and the hat cap is not local buckling critical (see Sketch b). For this case the assumption that the intersections of the elements of the hat are simply supported is a good approximation for local buckling calculations of the web and skin elements.

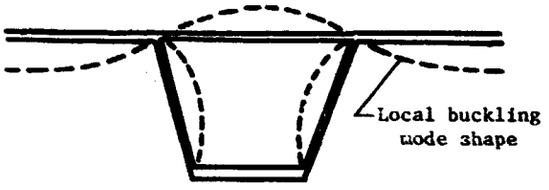

Sketch b

Minimum weight configuration B designs for more heavily loaded ($N_x/L > 200$ lb/in^2) compression panels typically have b/t ratios of the hat cap and skin under the hat, which are much lower than the b/t of the vertical webs or the skin between hats. In this case, the assumption that each of the hat elements are simply supported at their intersections was found to be overly conservative. Designs studied with BUCLASP-2 show a typical panel to buckle locally in a mode shape similar to that illustrated in Sketch c. For structures designed for $N_x/L > 200$ lb/in^2, large concentrations and thicknesses of 0° plies are required and a joint stiffening effect increases the local buckling load. In this case the web lateral edge boundary condition was found to be between simple support and clamped. The results presented in Figure 2 illustrate the additional load capability afforded by this improvement. A four-ply ($\pm 45/\mp 45$) laminate, for example, with clamped boundary condition will buckle at a load 59% higher than if the element were simply supported.

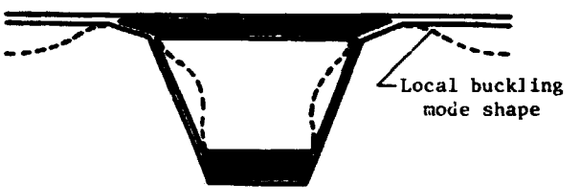

Sketch c

The current design program uses simple support boundary conditions for element local buckling and the advantage mentioned above has not yet been incorporated. The additional restraint offered by relatively thick hat caps and skin under the hat was studied, however, by increasing the depth of the web element of a synthesized design. Results of this study are presented in a subsequent section.

Residual Thermal Strains. The coefficient of thermal expansion for a laminate composed of 0° and $\pm\theta$ plies can vary widely. Hat cap and skin elements consisting of large concentrations of 0° plies, for example, have a much smaller coefficient than do web elements consisting of $\pm 45°$ plies. As a consequence, residual thermal strains exist at room temperature in a panel which was cured (i.e., was stress free) at an elevated temperature. Residual thermal strains may have both beneficial and detrimental effects. One effect of residual thermal strain for hat-stiffened panels is to put a prestressed tension field in the web elements at room temperature which must be relieved before the element can buckle. Simultaneously, a self-equilibrating compressive field exists in the hat cap and skin. A comprehensive study of these residual thermal strain effects on local buckling has not been conducted and residual thermal effects are not considered in the current design program.

Panel Warping. A further result of residual stresses is to develop warping along the panel length. Initial curvatures of this type can significantly degrade the structural performance of wide-column panels.[13] A methodology for effectively accounting for this phenomenon was not developed in the present program.

Test Specimens

Materials

Specimens tested in this investigation were fabricated using Thornel 300 graphite/Narmco 5208 epoxy in either tape or fabric form. Elastic properties of these materials used for design and analysis purposes are presented in Table II. The preliminary properties for graphite/epoxy tape defined in set 1 of Table II were used for the design of initial test specimens. Subsequent additional material testing indicated the material properties defined in set 2 to be more accurate. Subsequent panels and all of the design curves presented in this paper use the elastic properties defined in set 2.

Fabrication Technique

Specimens 60 inches long and up to 30 inches wide were manufactured using the fabrication technique illustrated in Figure 4. An aluminum tool was machined with the required hat or corrugation stiffener cross-sectional dimensions. The $\pm\theta$ web and 0° skin plies were laid into the mold after which a trapezoidal-shaped silicone rubber insert was positioned in the mold and the skin plies were laid on top. This layup was covered by a 0.25-inch-thick aluminum caul plate and the entire assembly was bagged for curing in an autoclave as shown in Figure 4(b). The silicone rubber inserts had a hole along their length which permitted autoclave pressure to be applied inside the hat stiffeners.

Specimen Description

Nine designs generated using the panel synthesis program were selected for fabrication and test. Characteristic features of these nine designs are presented in Table III and dimensions b_i and thicknesses t_i are listed in Table IV. Twenty-three specimens 16 inches long were used in local buckling studies and six specimens 60 inches long were built to evaluate Euler and modal interaction responses.

Designs A-1 through A-6 are hat-stiffened, configuration A, constructions; designs B-1 and B-2 are hat-stiffened, configuration B, constructions in which 0° plies in the skin are located only under the hat and not in the skin between stiffeners (i.e., $t_4 = 0$); and design C-1 is an open corrugation, configuration C, construction. The load

REPRODUCIBILITY OF THE
ORIGINAL PAGE IS POOR

index N_x/L is 100 lb/in^2 for hat-stiffened designs A-1 through A-5; 300 lb/in^2 for hat-stiffened designs A-6, B-1, and B-2; and 30 lb/in^2 for the open corrugation design C-1. Cross-sectional layup patterns for designs A-5 and B-2 are shown in Figure 5 and photographs of selected specimen cross sections are presented in Figure 6.

As indicated earlier, the automated program used to design specimens was modified several times during the course of this investigation. For specific designs, Table III indicates whether anisotropic or orthotropic plate theory was used for local buckling, if transverse shear effects were included, and the set of material properties used. The $\pm\theta$ orientation angle for most designs was taken to be 45°. Design A-2 and A-3 specimens, however, were constructed with the same mold used to fabricate design A-1 specimens with orientation angles of 52° and 60°, respectively. Design A-4 specimens were also fabricated in the same mold used to fabricate design A-1 specimens, but graphite/epoxy fabric was used as the $\pm$45° material.

Design B-1 is a variation of design A-6 in which the 0° plies in the skin are redistributed under the hat rather than between stiffeners. The Euler bending stiffness of design B-1 is less than that of design A-6 since the stiffener depth was maintained, but the 0° plies were moved closer to the stiffener neutral axis. Based on BUCLASP-2 results, the web depths of design B-2 were increased over the depth given by the synthesis program to take advantage of the additional restraint afforded the web by the relatively thick hat cap and skin.

Fabrication Related Problem Areas

During this investigation several problem areas which can reduce the predicted structural efficiency of the composite panels became evident. A discussion of these problem areas is presented in the following sections.

Laminate Material Properties. The elastic properties of a composite material can exhibit relatively large variations. Parametric studies showed that the synthesis program can reconfigure a hat-stiffened panel cross section to accommodate relatively large differences in material properties with only minor weight penalties. However, a configuration constructed of a material with properties different from those used in the design may be prematurely critical in local buckling. The severity of this problem is illustrated using results for design C-1. This configuration was designed using preliminary properties initially established for Thornel 300/5208 (set 1 listed in Table II). Subsequent to the panel design and fabrication, additional material testing indicated the properties listed under set 2 in Table II. This difference resulted in the open corrugation panel web being theoretically critical in local buckling at a strain 26% lower than that calculated using the initial properties. The sensitivity of local buckling to variations in the material properties makes it necessary to establish accurately composite material properties.

Material Thickness Variations. For design purposes, the thickness of a ply of Thornel 300/5208 material was assumed to be 0.0055 inch. The local ply thickness of the initial specimens reported in this paper were found to vary from -10% to +35% from this value. Improved fabrication techniques have reduced deviations from the design thickness of critical elements to $\pm$5%. In addition to having obvious direct effects on the weight of compression panels, ply thickness variations affect the load at which panel elements buckle. If it is assumed that the membrane stiffnesses are equal for two laminates composed of identical numbers and orientations of plies but different thicknesses, then the ratio of the buckling loads of the two laminates varies as the square of the ratio of their thicknesses. A 20% increase in thickness, for example, will result in a 44% increase in the local buckling load.

Closely related to the problem described above is the manner in which material property test data are reduced and used in structural design. Material property data should be established and reported in conjunction with a reference thickness. It is important that the elastic properties and ply thicknesses assumed in the design be reproduced as closely as is practical in the fabricated structure. This is necessary since deviations in either the membrane or bending stiffnesses may make the structure fail prematurely.

Specimen Weight Growth. Many of the specimens described in this report are heavier than the design prediction as a result of factors which were not considered in the minimum weight design but which developed during the design finalization and fabrication phases. In addition to the thick laminate problem described above, detailed design features (illustrated in Fig. 5) contributed to the panels being heavier than the weight predicted by the design program. For example, cutting and overlapping the $\pm\theta$ material in the hat cap added 2% to the weight of the panel for design A-5. For design B-2 interspersing 0° and $\pm$45° plies added four extra $\pm$45° plies to the skin under the hat and to the hat cap. These extra $\pm$45° plies added 9% to the weight of these specimens. The extra plies of material in design B-2 result in continuous filaments on the inside of the hat and around the interior fillet as shown in Figure 5. The layup sequence used in design A-5 required a fiberglass insert to reinforce the element intersection. The fiberglass insert used on design A-5 resulted in a 6% weight penalty.

Thus, it can be seen that seemingly insignificant alterations which are incorporated to improve fabricability or to improve a preliminary design can significantly reduce the theoretical structural weight efficiency. Closer attention to these weight problems has resulted in recently constructed panels which have been only 5% heavier than the idealized synthesis model. To achieve this improvement, close laminate thickness tolerance was maintained, the hat cap overlap was reduced to 0.5 inch, and a lighter weight fiberglass insert was used.

Experimental Instrumentation and Test Procedure

The 16-inch-long buckling specimens were axially compressed in a hydraulic test machine with a 300,000-pound capability (see Fig. 7). Strain gages were used to measure axial and transverse strains in each of the four hat stiffener elements. The crosshead movement and lateral displacements of

the panel were measured using a direct current differential transformer (DCDT). Strains, displacements, and the compressive load were recorded on magnetic tape and selected measurements were monitored during the test on an oscilloscope.

The moiré method for observing lateral displacements[14] was used to observe the buckle patterns as they developed during loading. Moiré fringe lines are lines of constant lateral displacement and therefore provide a contour map of the buckled mode shape. The basic instrumentation for this purpose involves a high-intensity light source, a moiré grid of 50 to 100 lines per inch, and a camera to record the fringe pattern for selected loads.

Specimen ends were potted into a 1-inch-thick block of epoxy and the ends were ground flat and parallel. To insure that the specimen was loaded uniformly, final adjustments were made by preloading the specimen to a small percentage of the ultimate load, then adjusting the crosshead platen until all axial strain gages on the stiffeners displayed approximately the same reading.

A similar procedure was used to test the 60-inch-long Euler buckling specimens. These specimens were loaded using a 1.2-million-pound capacity test machine.

Experimental Procedure for Defining Local Buckling

The critical load and strain at which panels exhibited local buckling was defined using the load/strain response and the strain reversal technique. Strain gages mounted on each of the four hat-stiffener basic cross-sectional elements (skin under the hat, web, hat cap, and skin between stiffeners) permitted identification of the element first exhibiting local buckling. The strain reversal technique which uses discrete strain measurements was complemented by the moiré fringe method to provide definition of the buckled mode shape.

Test Configuration Width and Lateral Boundary Condition

The BUCLASP-2 branched plate buckling program was used to determine the panel width and unloaded edge boundary conditions required to experimentally study panel buckling behavior. Analytical results showed that a two-stiffener-wide panel was adequate and would give the same results as wider panels. Studies also showed that it was necessary to either support the panel unloaded edge or to cut back the free edge of element 4 to prevent its local buckling. Since testing with a free edge is less complicated, hat-stiffened panels were tested in a reduced width configuration. BUCLASP-2 results showed it was necessary, however, to test open corrugation specimens using a lateral support.

Results and Discussion

Local Buckling Experiments

A summary of the results of experiments on 23 local buckling specimens is presented in Table V. Results for two or more specimens are included for each of the designs defined in Table III. Ultimate strength as well as local buckling stress resultant and strain information is tabulated. In addition, the first element of the panel cross section to exhibit local buckling is indicated. The panel reduced width is presented for each specimen. All but two of the hat-stiffened panels were tested in a two-stiffener-wide configuration. Two of the specimens of design A-4 were three stiffeners wide. Open corrugation specimens (design C-1) were tested in a full three-bay width with knife-edge lateral supports.

The skin between stiffeners (element 4) was experimentally found to buckle first for designs A-2 through A-6. The skin under the stiffener and the web either buckled simultaneously with element 4 or at slightly higher loads. The hat cap did not exhibit local buckling for any of the hat-stiffened compression test panels, which is consistent with the design prediction. The open corrugation panel (design C-1) exhibited simultaneous local buckling of all elements. Specimens of design B-1 failed without exhibiting local buckling. Specimen of design B-2 buckled locally in the web but did not exhibit buckling of other cross-sectional elements.

A graph of the stress resultant as a function of the imposed strain for the axially oriented strain gages mounted on one of the design A-2 specimen ($\theta = 52°$) is presented in Figure 8. Bending effects caused by local imperfections or specimen alinement are probably responsible for the divergence of back-to-back gages beginning at the origin. Local buckling of the skin between stiffeners (element 4) was found to occur at an axial load of 3295 lb/in. as shown in Figure 8. Moiré fringe patterns for selected loads applied to the same specimen are presented in Figure 9. The moiré fringe shows the development of local buckling of element 4 at loads around 3030 lb/in. Comparison of strain reversal and moiré fringe results indicates the development of local buckling of the skin under the hat (element 1) at slightly higher loads than for the skin between stiffeners. Thickness variation along the panel length may account for the biased development of buckling fringe patterns at one end of the panel. At a load of 4166 lb/in., the eight buckling half waves are clearly developed for the 16-inch-long panel. The corresponding number of half waves for design A-1 specimens ($\theta = 45°$) and design A-3 specimens ($\theta = 60°$) was 6 and 10, respectively.

Comparison of the magnitude of local buckling and ultimate loads (Table V and Fig. 8) indicates that some test specimens exhibited the capability to carry loads beyond the onset of local buckling. However, current specimens were not designed to utilize post-buckling behavior. Some specimens exhibiting post-buckling behavior failed at loads less than the design load. All elements are depended upon to carry loads in proportion to their initial axial stiffness. Theoretically, for long specimens, the coincidence of local buckling and Euler buckling initiates failure. While the results herein indicate that buckled skin concepts might be possible, the brittle nature of graphite/epoxy composites makes their practicality highly speculative at this time.

Local buckling specimens failed ultimately in one of the two manners illustrated by the photographs of Figures 10 and 11. Failures of specimens

of design A-1 through A-6 are characterized by Figure 10. The hat cap is broken and the skin is delaminated and separated from the web. Specimens of design B-1 and B-2 ultimately failed in an explosive fashion. The stiffener detached from the skin and a large amount of material was separated into small splinters as seen in the photograph of Figure 11.

The ultimate failure of specimens of designs B-1 and B-2 were at relatively high strains and exceeded the Euler design strain by 47% and 29%, respectively. Specimens of designs A-1 through A-5, which failed at strains greater than 0.007 in./in., exhibited, in a limited fashion, some explosive failure characteristics. It is not known whether the type of failure is related to the configuration (A or B) or to the fact that configuration B specimens were more heavily loaded (N_x/L = 300 lb/in^2) and resulted in thicker concentrations of 0° plies in the hat cap and skin under the hat. Specimen, of design A-6 have been discounted in this observation since these specimens failed at relatively low axial strains.

BUCLASP-2 Analytical Model

Modeling of a structure composed of thick hat cap and skin elements such as designs B-1 and B-2 was examined to determine the best analytical representation. A less accurate representation will result if the element junctures are not carefully specified since local buckling is directly related to the element width. For BUCLASP-2 the element width is the distance between grid points. The two models formulated for designs B-1 and B-2 presented in Figure 12 illustrate this problem. The difference in the two models is the width of the web (element 2). For model I the width of element 2 is the dimension from the point of contact with element 1 to the point of contact with element 3. For model II this width is the dimension from the center line of the element which represents the 0.35-inch tapered skin region (see Fig. 1) to the center line of the hat cap. Elements are offset for both models to permit correct representation of the overall bending stiffness. Differences of 24% and 29%, respectively, were obtained for the local buckling load for designs B-1 and B-2 using these two models as shown in Figure 12. Model I, which yielded the higher solution, is considered the better representation. Results presented in this paper use model I to represent cross sections composed of thick laminates. The two models converge to approximately the same solution for designs composed of thin laminate elements.

Experimental and Analytical Comparison

Analytical results for the local buckling of test panel designs obtained using BUCLASP-2 are presented in Table V. Calculations are based on nominal design dimensions and thicknesses presented in Table IV.

A comparison of experimental and BUCLASP-2 results for local buckling is presented in Figure 13. The agreement is good for some configurations and poor for others. Part of the lack of correlation is because BUCLASP-2 does not account for anisotropic or residual thermal strain effects and all results are based on nominal thicknesses. Critical elements for designs A-1, A-2, A-3, and A-5 were thicker than the nominal design thickness which increased their test results. Conversely, specimens of design A-6 were found to be thinner than the nominal which decreased their buckling loads. The web depth dimension for design B-2 was intentionally increased over the initial design value. This increased the Euler buckling capability but also made the four-ply ($\pm$45/$\mp$45) web laminate the only element critical in local buckling for this design.

For design purposes, it was assumed that local buckling is independent of panel length and modal interaction is ignored. The validity of this assumption was studied using BUCLASP-2. Analytical results from BUCLASP-2 for designs A-1 (θ = 45°), A-2 (θ = 52°), and A-3 (θ = 60°) are presented in Figure 14, which shows the panel critical strain as a function of panel length. These results show the local buckling loads for design A-1 to be constant for panel lengths less than 25 inches, the interactive modes to dominate for lengths from 25 to 32 inches, and the Euler modes to be critical for longer length panels. Similar results were obtained for designs A-2 and A-3. The local buckling critical strain for design A-2 is higher and the value for design A-3 is lower than the critical strain for design A-1. Modal interaction reduces by 12% the buckling strain capability of a design determined by the intersection of the BUCLASP-2 local and Euler buckling curves.

Local buckling experimental results are also presented in Figure 14. Local buckling critical strains were higher for specimens of designs A-2 and A-3 than for specimens of design A-1. Thick laminates account for part but not all of the discrepancy between experimental and BUCLASP-2 results. The BUCLAP2 anisotropic plate solution for the critical strain of the web and skin under the hat of design A-1 adjusted for a 20% thick laminate is 0.004 in./in. This analytical result is in good agreement with experimentally determined values.

Residual thermal strains may have an effect on local buckling, but the importance has not been thoroughly examined. The magnitude of residual strains in the web of specimens of designs A-1 and A-2 were experimentally measured. Strain gages mounted on the web were read before and after the web was cut from the stiffener. An axial residual tensile strain of 0.0001 and 0.0008 in/in., respectively, existed in the web of specimens of designs A-1 and A-2 prior to its removal. This residual tensile strain must be relieved before compressive strains are imposed on this element. This effect may partially account for the high experimental results indicated in Figure 14.

The design assumption of requiring local and Euler buckling to occur simultaneouly and ignoring modal interaction was also evaluated using BUCLASP-2 for a design which included thick hat cap and skin elements (design B-1). The buckling strain for design B-1 plotted as a function of the panel length is presented in Figure 15. The buckling strain is observed to be a continuously decreasing function of the panel length. Local buckling modes are critical for lengths less than 8 inches, modal interaction is critical for lengths between 8 and 25 inches, and the Euler mode is critical for lengths greater than 25 inches. The local mode is characterized by lateral displacements of the webs.

ORIGINAL PAGE IS POOR

The buckling strain of the web was also calculated for simple support or clamped lateral edge boundary conditions and with orthotropic and anisotropic theory using BUCLAP2. It is observed that BUCLASP-2 results for the local buckling strain, based on orthotropic theory, agrees with the BUCLAP2 orthotropic solution with clamped lateral edges of the web. This result indicates that the thick hat cap and skin elements provide clamped edge support to the thin four-ply web. For this type of panel, a design based on simple support anisotropic plate theory for local buckling which also meets Euler buckling requirements is a conservative design.

The experimental data for local buckling of specimens of design B-1 plot higher than the theoretical results. The fact that cross-sectional elements were thicker than the nominal design thickness by approximately 10% partially explains this discrepancy. The specimens failed without exhibiting local buckling.

Compression Panel Structural Efficiency

A theoretical comparison of the relative structural efficiencies of graphite/epoxy and aluminum compression panels is presented in the logarithmic graph of Figure 16 in which panel weight per unit area per unit length (W/AL) is plotted as a function of the load index (N_x/L). These curves were generated by the compression panel design program used in this study, the constraints defined in Table I, and property sets 2 and 4 listed in Table II. Graphite/epoxy results are presented for a hat-stiffened panel (Fig. 1) and for an open corrugation panel (configuration C). The ply orientation angle θ was taken to be 45°. The cusps of the curve correspond to imposing the constraint that $\pm 45°$ material is used in sets of four symmetric plies. It was found that the design program could reconfigure the cross section so that very little weight penalty resulted from the further requirement that the thicknesses t_3, t_4, and t_5 must also be discrete. The discrete thickness cusps shift relative positions depending on the panel design length. For the purposes of this study, a panel length of 30 inches was selected. Open corrugation panels were found to be approximately 20% lighter than hat-stiffened panels and graphite/epoxy hat-stiffened panels are approximately 50% lighter than comparably designed aluminum hat-stiffened panels.

Test results for 60 inch long buckling specimens constructed using designs A-1, A-2, A-4, A-5, B-2, and C-1 are presented in Table VI and are also shown in Figure 16. A photograph of one of these test panels is presented in Figure 17. Hat-stiffened panels were tested with clamped boundary conditions on the loaded ends and with the lateral edges unsupported. The effective simple support length of test panels was defined using strain-gage data and the data reduction technique described in Reference 15. This length was found to be approximately 31 inches for a 60-inch-long clamped end panel. For the hat-stiffened panels, the skin element free edge was reduced in width to circumvent its premature buckling. The open corrugation panel was tested with knife-edge lateral supports in a full width configuration. The actual test panel width was used in calculations of the stress resultant N_x for all panels except specimen B-2. Since only a small percentage of the total stiffness for specimen B-2 was in the skin between stiffeners, the panel width was based on the typical stiffener spacing. Critical loads for three of the panels (A-1, B-2, and C-1) are ultimate values since these panels were tested to destruction. Alternate load conditions are planned for panels A-2, A-4, and A-5 and therefore loading on these panels was terminated short of the ultimate, and the critical load was extrapolated from test data using the force/stiffness method described in Reference 16.

The initial curvature which existed in each of the test panels is also presented in Table VI. The maximum deviation at the center of the panel from a straight line drawn through the ends of the 60-inch-long specimens varied from 0.005 inch for the open corrugation specimen C-1 to 0.100 inch for hat-stiffened specimens A-2 and A-4. The open corrugation specimen had almost negligible initial curvature since specimen C-1 has a symmetric cross section. The 0.100-inch initial curvature which existed in specimens A-2 and A-4 was sufficient to reduce the load capability of these panels by approximately 20%.

Experimental results are also presented in Figure 16 for nearly 2000 aluminum panels of hat, J and Y stiffened construction. Aluminum data are taken from NACA reports.[2-6] The minimum weight curve generated for aluminum hat-stiffened compression panels forms the lower bound for hat-stiffened panel experimental data. A few data points for the Y configuration (which is a more efficient configuration)[6] fall below the minimum weight curve for aluminum hat-stiffened panels.

Test results for graphite/epoxy hat-stiffened specimens are 32% to 42% lighter in weight than results for the best design available for similar aluminum panels (see Fig. 16). Although these results represent initial efforts, 64% to 84% of the theoretical weight reduction available for hat-stiffened composite compression members has been demonstrated. Results of this investigation indicate that most of the remaining theoretical weight savings are available if attention is given to the design and fabrication problem areas identified earlier in this paper. Improved fabrication techniques have subsequently been developed in which specimen weights closely match design weight estimates. Improved design and fabrication procedures which reduce the magnitude of thermally induced initial curvatures will permit composite panels to meet design load requirements.

The open corrugation composite panel test result is 58% lighter than the theoretical result for an aluminum hat-stiffened panel. The 812-lb/in. axial load carried by this panel represents 90% of the design load. This panel weighed only 0.312 lb/ft^2 which makes it an attractive candidate for lightly loaded structural applications which do not require a smooth surface.

Axial Stiffness of Minimum Weight Panels

Minimum weight panels studied in the current program are designed to efficiently carry axial compressive loads and an inplane stiffness requirement was not imposed. It is recognized that inplane stiffness is important for many structural applications.

It is of interest, therefore, to examine the axial stiffnesses which resulted for the minimum weight aluminum and graphite/epoxy compression panels presented in Figure 16. A logarithmic graph of the axial stiffness for these panels as a function of load index N_x/L is presented in Figure 18. Finite jumps occur in the axial stiffness at magnitudes of N_x/L for which the minimum weight panel changes values of t_1 and t_2 (see Fig. 16).

The minimum-weight graphite/epoxy axial stiffness fluctuates between being less stiff and more stiff than the corresponding minimum-weight aluminum panel. It is also seen that the option exists at load indices in regions where minimum-weight configurations changes values of t_1 and t_2 to have alternate panels with approximately the same weight but different axial stiffnesses. The design with the smaller value of t_1 and t_2 will be approximately twice as stiff as the design with the larger value of t_1 and t_2. This reflects a larger percentage of ± 45 oriented material for the less stiff design.

Concluding Remarks

Preliminary findings of an analytical and experimental program to establish a weight and strength data base for efficient graphite/epoxy compression panels of stiffened construction have been presented. A brief description of the constraints and design assumptions used in the panel design program is given as well as a discussion of a branched plate buckling analysis which was used for correlating analytical and experimental results. The results presented are for several hat-stiffened panel designs and for one open corrugation compression panel. Experiments were conducted on short specimens to study local buckling and ultimate strength, and on longer wide-column specimens which were used to evaluate Euler buckling and modal interaction.

Results from the theoretical design studies indicate that G/E hat-stiffened compression panels possess a weight savings on the order of 50% when compared with comparably designed aluminum compression panels. Weight savings of 32% to 42% were experimentally achieved in the current investigation. Realization of the full 50% weight savings potential will require close attention to design and fabrication details. Open corrugation graphite/epoxy designs were shown to be approximately 20% lighter than graphite/epoxy hat-stiffened designs. A 0.312-lb/ft^2 open corrugation specimen with a 31-inch simple support length experimentally carried an axial load of 812 lb/in. which is 90% of the theoretical potential.

A hat-stiffened panel having stiffener vertical webs composed entirely of $\pm 45°$ material with the 0° plies located in the hat cap and skin was shown to have high structural efficiency. Locating 0° plies in the skin directly under the hat cap and not in the skin between stiffeners was found to provide further structural efficiency gains for moderately loaded designs ($N_x/L > 200$ lb/in^2). This improved structural efficiency is a result of a boundary stiffening effect on the hat vertical webs from the thicker connecting hat cap and skin elements.

Differences in the coefficient of thermal expansion of web, hat cap, and skin elements of hat-stiffened composite structures can result in relatively large residual thermal stresses from the curing process. These thermal stresses can cause panel thermal warping and may affect the local buckling behavior. Correlation between analytical and experimental results in this investigation is marginal as a consequence of variations in laminate thicknesses, anisotropic effects, and the above-mentioned residual thermal stresses which were not accounted for in the analysis.

The preliminary results presented herein for controlled tests have identified important areas in which further research must be conducted if rational design methods are to be developed for efficient composite compression panels. Among these are (1) the development of a design capability which properly accounts for the different thermal strains which occur as a consequence of elevated temperature curing, (2) the development of a special-purpose anisotropic branched plate buckling analysis which can account for coupled modes, and (3) the establishment of a rationale for determining elastic properties and material allowables which will enable their consistent use throughout the design, experimental and analytical phases of a composite structures development program.

The design studies conducted during the course of this program indicated that smaller weight penalties will result if performance degrading effects such as transverse shearing deformations, anisotropic effects, and thermal warping are taken into account early in the design cycle, rather than considering them later. It was also observed that the panel extensional stiffness could vary by as much as a factor of 2 for two different panels which have weights approximately the same. This result indicates that structural stiffness should also be considered early in the design cycle.

References

[1]Peterson, James P., "Structural Efficiency of Aluminum Multiweb Beams and Z-Stiffened Panels Reinforced With Filamentary Boron-Epoxy Composite," TN D-5856, 1970, NASA.

[2]Schuette, Evan H., Barab, Saul, and McCracken, Howard L., "Compression Strength of 24S-T Aluminum-Alloy Flat Panels With Longitudinally Formed Hat-Section Stiffeners," TN 1157, 1946, NACA.

[3]Hickman, William A., and Dow, Norris F., "Compressive Strength of 24S-T Aluminum-Alloy Flat Panel With Longitudinal Formed Hat-Section Stiffeners Having Four Ratios of Stiffener Thickness to Skin Thickness," TN 1553, 1948, NACA.

[4]Hickman, William A., and Dow, Norris F., "Data on the Compressive Strength of 75S-T6 Aluminum-Alloy Flat Panels, Having Small Thin, Widely Spaced, Longitudinal Extruded Z-Section Stiffeners," TN 1978, 1949, NACA.

[5]Hickman, William A., and Dow, Norris F., "Data of 75S-T6 Aluminum-Alloy Flat Panels With Longitudinal Extruded Z-Section Stiffeners," TN 1824, 1949, NACA.

[6]Dow, Norris F., and Hickman, William A., "Design Charts for Flat Compression Panels Having Longitudinal Extruded Y-Section Stiffeners and Comparison With Panels Having Formed Z-Section Stiffeners," TN 1389, 1947, NACA.

[7]Agarwal , B. L., and Davis, R. C., "Minimum-Weight Designs for Hat-Stiffened Composite Panels Under Uniaxial Compression," TN D-7779, 1974, NASA.

[8]Viswanathan, A. V., and Tamekuni, M., "Elastic Buckling Analysis for Composite Stiffened Panels and Other Structures Subjected to Biaxial Inplane Loads," CR-2216, 1973, NASA.

[9]Tripp, L. L., Tamekuni, M., and Viswanathan, A. V., "User's Manual-BUCLASP-2. A Computer Program for Instability Analysis of Biaxially Loaded Composite Stiffened Panels and Other Structures," CR-112226, 1973, NASA.

[10]Halstead, David W., Tripp, L. L., Tamekuni, M., and Baker, L. L., "User's Manual BUCLAP2. A Computer Program for Instability Analysis of Laminated Long Plates Subjected to Combined Inplane Loads," CR-132298, 1973, NASA.

[11]Ashton, J. E., Halpin, J. C., and Petit, P. H., Primer on Composite Materials Analysis, Technomic Publishing Co., Inc., 1969.

[12]Bleich, Friedrich, Buckling Strength of Metal Structures, McGraw-Hill Book Company, 1952, p. 24.

[13]Giles, Gary, and Anderson, Melvin S., "Effects of Eccentricities and Lateral Pressure on the Design of Stiffened Compression Panels," TN D-6784, 1972, NASA.

[14]Dykes, B. C., "Analysis of Displacements in Large Plates by the Grid-Shadow Moiré Technique," Fourth International Conference on Experimental Stress Analysis, Cambridge, England, 1970.

[15]Schuette, Evan H., and Roy, J. Albert, "The Determination of Effective Column Length From Strain Measurements," Wartime Report, ARR No. L4F24, 1944, NACA.

[16]Jones, Robert E., and Greene, Bruce E., "The Force/Stiffness Technique for Nondestructive Buckling Testing," AIAA/ASME/SAE 15th Structures, Structural Dynamics, and Materials Conference. Las Vegas, Nevada, April 1974, AIAA Paper No. 74-351.

TABLE I. UPPER AND LOWER BOUNDS ON GEOMETRIC CONSTRAINTS AND STRAIN

Constraint*	Graphite/epoxy (Thornel 300/5208)	Aluminum
t_1, t_2	Integer sets of four symmetric plies	$\geq$0.005 in.
t_3, t_4, t_5	$\leq$0.25 in.	None
b_1, b_3	$\geq$0.8 in.	$\geq$0.8 in.
b_2, b_4	$\geq$0.8 in.	$\geq$0.1 in.
ε_x	$\leq$0.009 in./in.	$\leq$0.0068 in./in.

*See Figure 1 for geometry definitions.

TABLE II. MATERIAL ELASTIC PROPERTIES

Set number	Material	E_1, Mlb/in^2	E_2, Mlb/in^2	G_{12}, Mlb/in^2	ν_{12}	ρ, lb/in^3
1	Thornel 300/5208 unidirectional tape	21.0	2.39	0.65	0.314	0.055
2	Thornel 300/5208 unidirectional tape	19.6	2.1	0.76	0.314	0.055
3	Thornel 300/5208 balanced fabric	9.0	9.0	0.65	0.010	0.055
4	Aluminum	10.5	10.5	3.95	0.330	0.100

TABLE III. TEST PANEL DESIGN CHARACTERISTICS

Design§	Design features*						Number of 16-inch specimens	Number of 60-inch specimens
	$\frac{N_x}{L}$, lb/in^2	$\frac{W}{AL}$, lb/in^3	Anisotropic (A) or orthotropic (O) laminate theory	Transverse shear effects included	Material properties used in design**	Ply orientation angle θ, deg		
A-1	100	0.000153	O	No	1	45	3	1
A-2†	100	0.000153	O	No	1	52	3	1
A-3†	100	0.000153	O	No	1	60	2	0
A-4†	100	0.000192	O	No	1, 3	45 (fabric)	4	1
A-5	100	0.000157	A	Yes	1	45	2	1
A-6	300	0.000257	O	No	1	45	3	0
B-1	300	0.000254	O	No	1	45	2	0
B-2	300	0.000260	A‡	Yes	2	45	2	1
C-1	30	0.0000719	A	No	1	45	2	1

*Designs based on L = 30 inches.

**See Table II for property set definitions.

†Configuration dimensions are the same as design A-1 thus the design is not necessarily of minimum weight.

‡Web depth increased based on BUCLASP-2 studies.

§See Sketch a.

TABLE IV. NOMINAL COMPRESSION PANEL DIMENSIONS AND THICKNESSES*

Design	b_1, in.	b_2, in.	b_3, in.	b_4, in.	t_1, in.	t_2, in.	t_3, in.	t_4, in.	t_5, in.
A-1	1.320	1.349	0.800	1.016	0.022 (4)**	0.022 (4)	0.066 (12)	0.0165 (3)	0
A-2	1.320	1.349	0.800	1.016	0.022 (4)	0.022 (4)	0.066 (12)	0.0165 (3)	0
A-3	1.320	1.349	0.800	1.016	0.022 (4)	0.022 (4)	0.066 (12)	0.0165 (3)	0
A-4	1.320	1.349	0.800	1.016	0.030 (2)	0.030 (2)	0.066 (12)	0.0165 (3)	0
A-5	1.242	1.218	0.800	1.101	0.022 (4)	0.022 (4)	0.066 (12)	0.022 (4)	0
A-6	1.178	1.391	0.800	1.175	0.022 (4)	0.022 (4)	0.2035 (37)	0.055 (10)	0
B-1	1.178	1.391	0.800	1.175	0.022 (4)	0.022 (4)	0.2035 (37)	0	0.0825 (15)
B-2	1.477	1.680	0.803	1.490	0.022 (4)	0.022 (4)	0.253 (46)	0	0.099 (18)
C-1	2.713	1.096	0.895	0.895	0	0.022 (4)	0.022 (4)	0.022 (4)	0

*See Figure 1 for dimension and thickness definitions.

**Number of plies.

TABLE V. LOCAL BUCKLING RESULTS FOR 16-INCH-LONG PANELS

Design	Experimental results						BUCLASP solution for local buckling**	
	Panel width,* in.	Ultimate		Local Buckling		Element first exhibiting local buckling		
		N_x,† lb/in.	$\bar{\epsilon}_x$, in./in.	N_x,† lb/in.	$\bar{\epsilon}_x$, in./in.		N_x,† lb/in.	$\bar{\epsilon}_x$, in./in.
A-1	5.32	3819	0.0050	2763	0.0036	2	3230	0.00443
A-1	5.32	3855	0.0048	3102	0.0040	1, 2, 4	3230	0.00443
A-1	5.21	3992	0.0056	2917	0.0041	4	3230	0.00443
A-2	5.28	4743	0.0063	3295	0.0048	4	3172	0.00461
A-2	5.28	5115	0.0077	4413	0.0065	4	3172	0.00461
A-2	5.28	4934	0.0073	4015	0.0057	4	3172	0.00461
A-3	5.31	5021	0.0074	4072	0.0060	1, 2, 4	2831	0.00419
A-3	5.31	5309	0.0074	3691	0.0054	4	2831	0.00419
A-4	5.24	5703	0.0076	4890	0.0063	4	5284	0.00700
A-4	5.26	5036	0.0063	4639	0.0057	2, 4	5284	0.00700
A-4	8.60	4826	0.0064	4535	0.0060	2	5087	0.00696
A-4	8.60	4535	0.0060	None	None	None	5087	0.00696
A-5	5.32	5103	0.0072	4192	0.0056	4	3120	0.00394
A-5	5.30	4283	0.0060	4019	0.0056	4	3120	0.00394
A-6	5.35	8402	0.0045	6168	0.0030	4	9724	0.00489
A-6	5.28	8352	0.0040	7008	0.0033	4	9724	0.00489
A-6	5.28	8236	0.0038	6440	0.0030	2	9724	0.00489
B-1	5.32	16900	0.0077	None	None	None	17556	0.00785
B-1	5.32	17430	0.0076	None	None	None	17556	0.00785
B-2	6.72	14590	0.0063	8209	0.0036	2‡	11752	0.00474
B-2	6.72	14440	0.0065	10896	0.0049	2‡	11752	0.00474
C-1	10.90	960§	0.0034	651	0.0023	2, 3	1173	0.00387
C-1	10.90	1008§	0.0034	688	0.0023	2, 3	1173	0.00387

*Specimen lateral edges reduced for free edge test condition.

**Calculations based on design dimensions and thicknesses listed in Table IV and material property Set 2 in Table II.

†N_x calculations based on test panel width.

‡Elements 1, 3, and 4 did not buckle during the test.

§Specimen lateral edges supported by knife edge.

REPRODUCIBILITY OF THE
ORIGINAL PAGE IS POOR

TABLE VI. TEST RESULTS FOR 60-INCH-LONG EULER BUCKLING SPECIMENS

Design		Experimental results					
Specimen	N_x, lb/in.	Panel width,* in.	N_x,** lb/in.	$\frac{N_x}{L_e}$,† lb/in^2	$\frac{W}{A}$, lb/ft^2	$\frac{W}{AL_e}$,† lb/in^3	Initial curvature,‡ in.
A-1	3000	18.75	1929	66.8	0.786	0.000176	0.060
A-2	3000	22.06	2130§	73.1	0.786	0.000176	0.100
A-4	3000	22.25	2214§	71.0	0.924	0.000207	0.100
A-5	3000	22.75	2447§	83.7	0.844	0.000189	0.040
B-2	9000	15.63	7630	246.2	1.295	0.000290	0.020
C-1	900	25.38‖	812	25.9	0.312	0.000070	0.005

*Specimen lateral edges reduced for free edge test condition.

**Test panel width used to calculate N_x except for specimen B-2 where width including removed edges was used (17.8 in.).

†Effective simple support length L_e experimentally found to be approximately 31 inches.

‡Maximum deviation at center of panel from straight line drawn through ends of 60-inch-long specimen.

§Critical load extrapolated from test data using force/stiffness technique.[16]

‖Specimen lateral edges supported by knife edge.

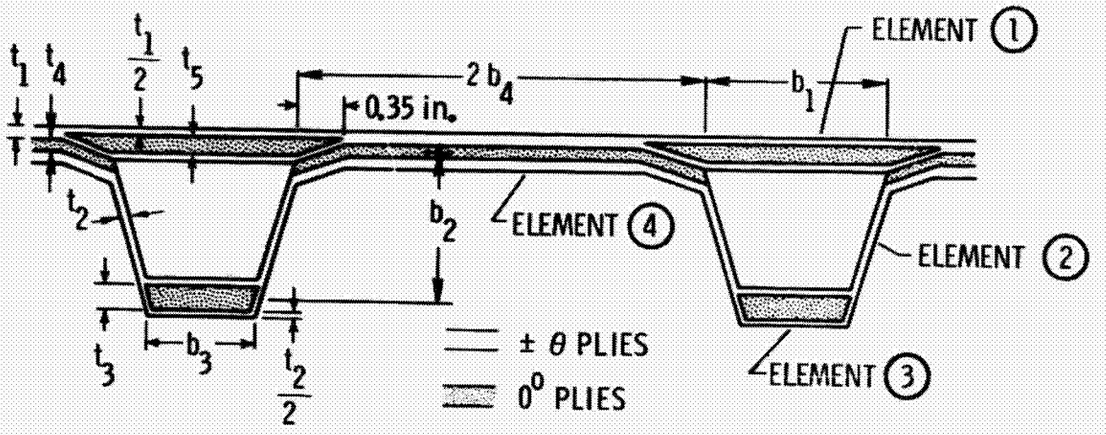

Figure 1. Hat-stiffened compression panel analytical model.

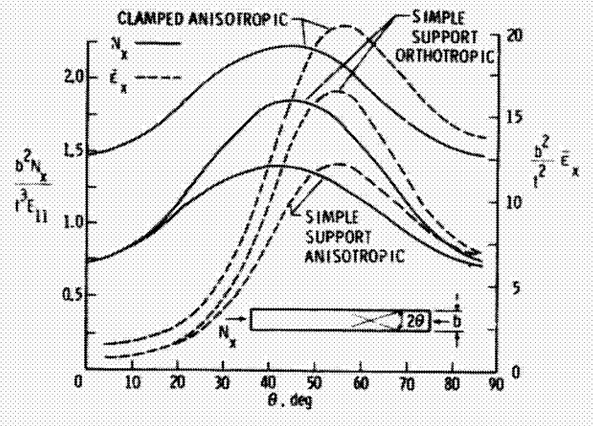

Figure 2. Effect on buckling load and strain of anisotropic versus orthotropic theory for four-ply (±45/∓45) laminate. Material properties used are set 2 listed in Table II.

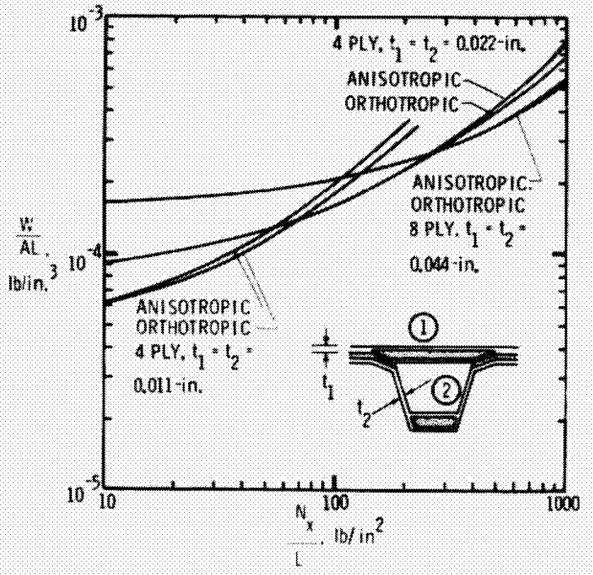

Figure 3. Weight efficiency penalty for imposing anisotropic constraints to hat-stiffened panel elements 1 and 2.

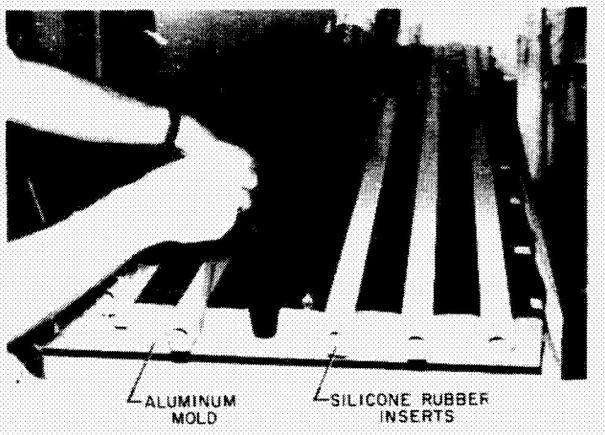

(a) Panel assembly

Figure 4. Fabrication process.

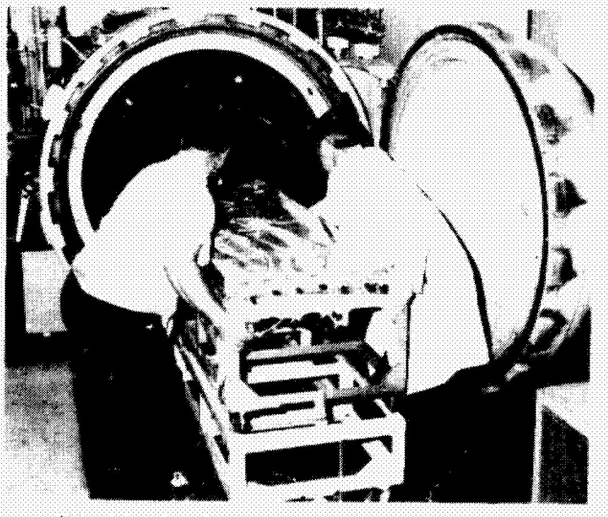

(b) Placing bagged specimen in autoclave.

(Figure 4. Concluded.

REPRODUCIBILITY OF THE ORIGINAL PAGE IS POOR

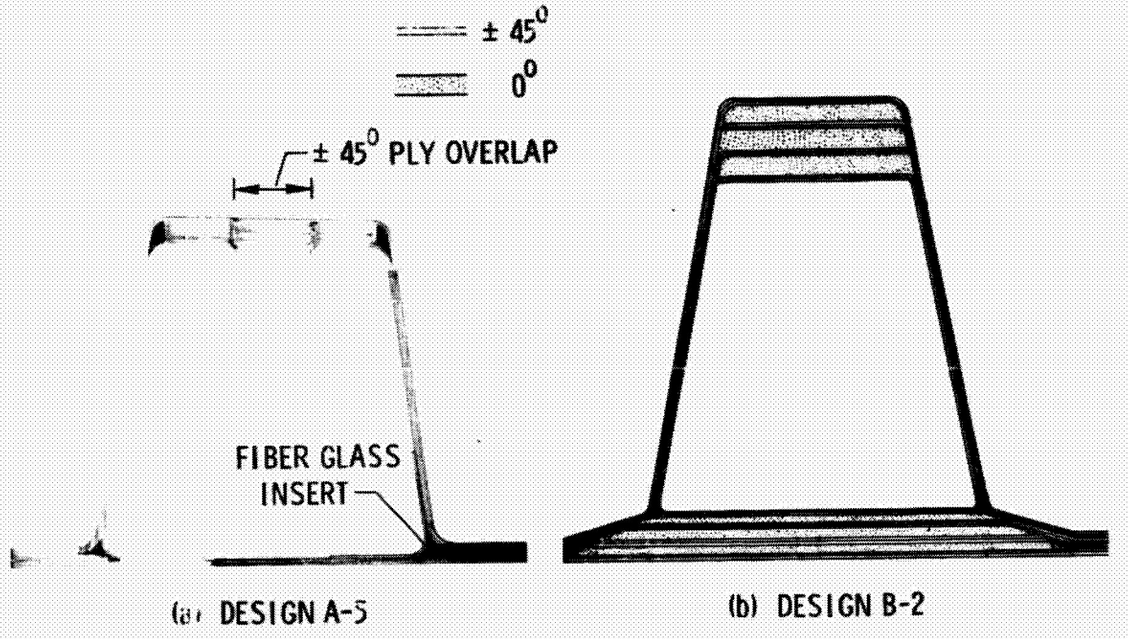

Figure 5. Fabrication drawings.

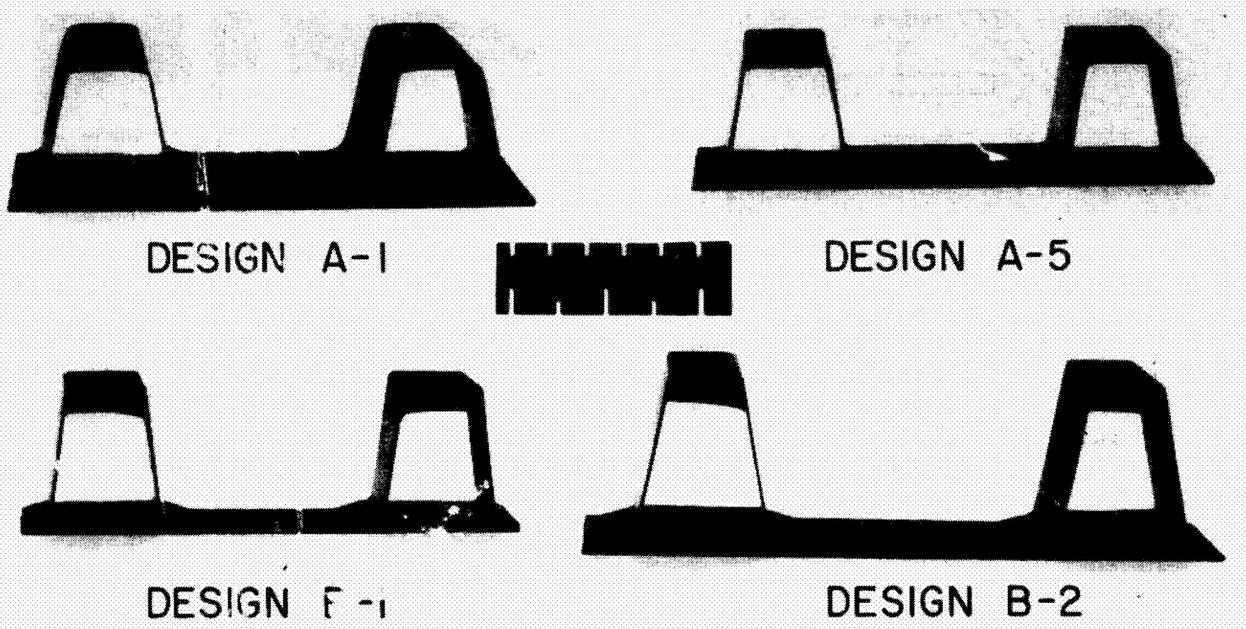

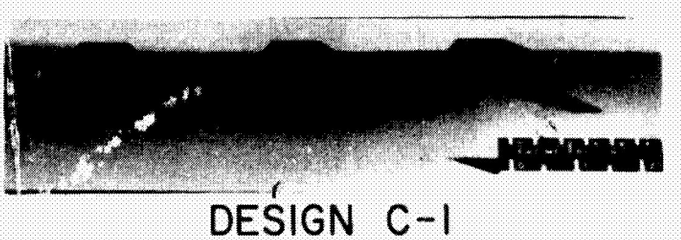

Figure 6. Photographs of selected design cross sections.

REPRODUCIBILITY OF THE
ORIGINAL PAGE IS POOR

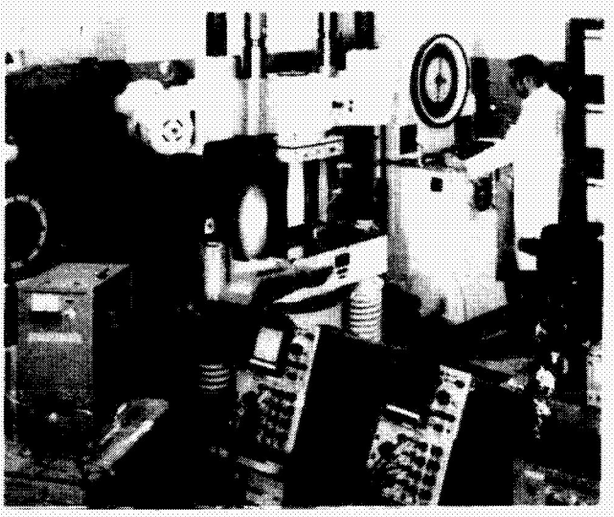

Figure 7. Test instrumentation.

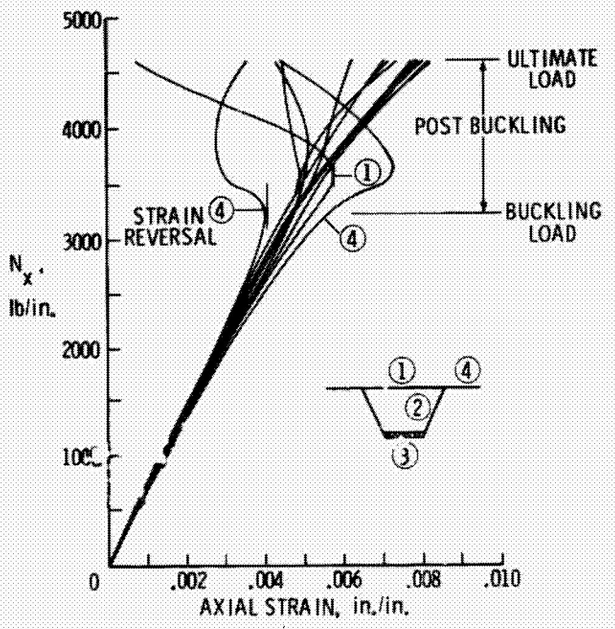

Figure 8. Stress resultant as a function of strain for axially oriented gages mounted on specimen of design A-2.

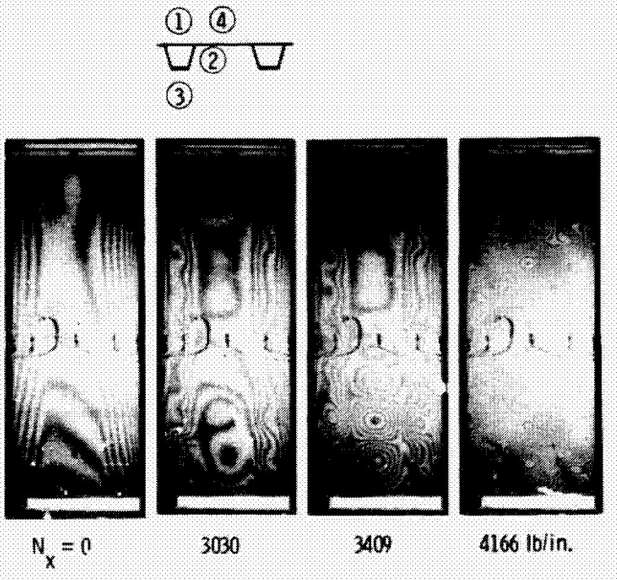

Figure 9. Moiré photographs of buckle pattern for specimen of design A-2.

REPRODUCIBILITY OF THE ORIGINAL PAGE IS POOR

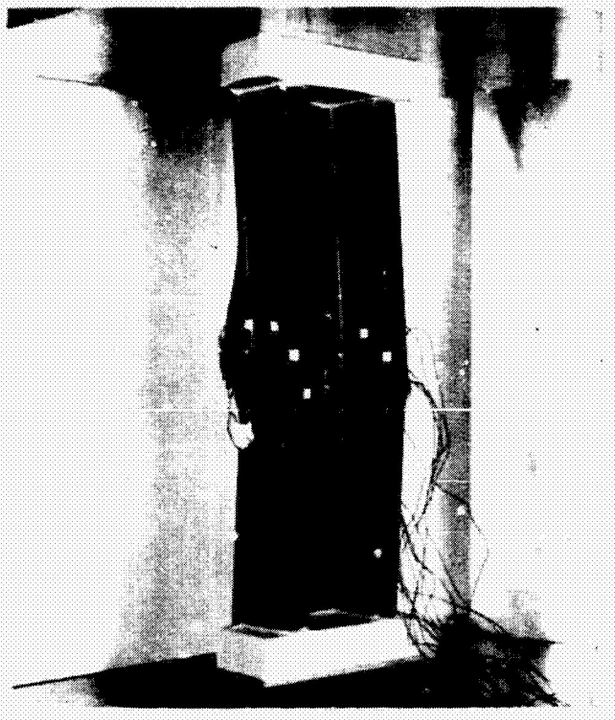

Figure 10. Failed specimen typical for moderately loaded (N_x/L = 100 lb/in^2) designs A-1 through A-5.

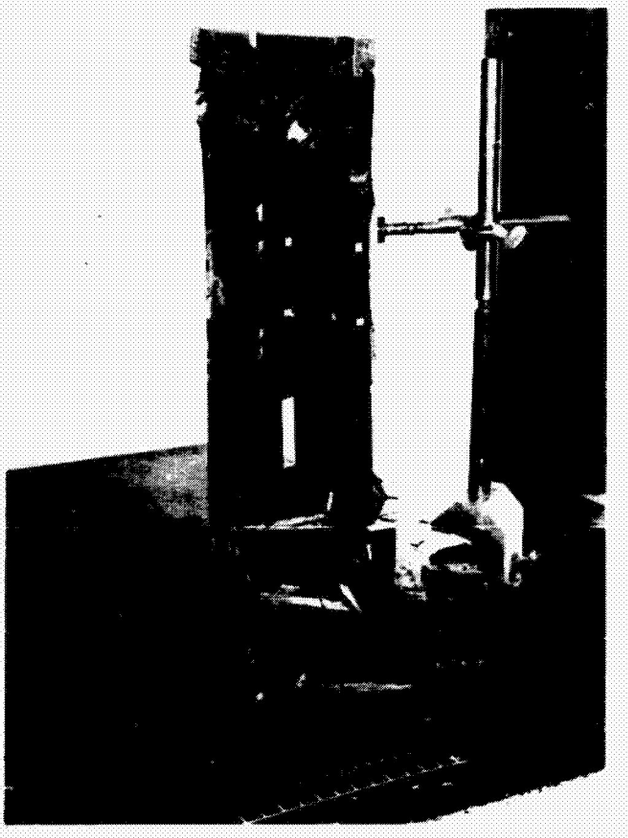

Figure 11. Failed specimen typical for heavily loaded (N_x/L = 300 lb/in^2 designs B-1 and B-2.

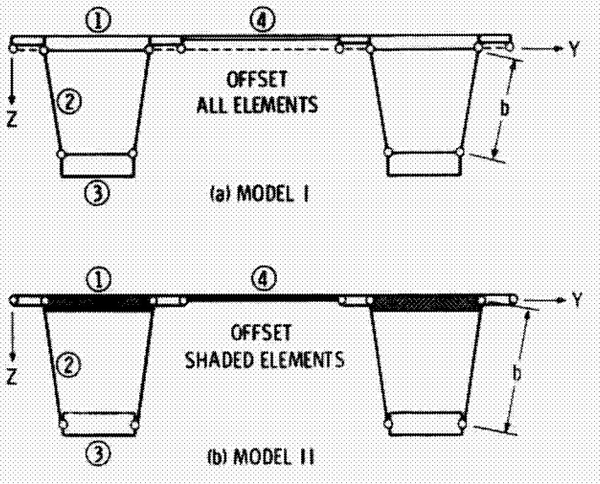

	N_x, lb/in.		$\bar{\epsilon}_x$, in./in.	
	Design B-1	Design B-2	Design B-1	Design B-2
Model I	17556	11752	0.00785	0.00474
Model II	12508	9007	0.00557	0.00362

Figure 12. BUCLASP-2 web modeling approaches.

REPRODUCIBILITY OF THE
ORIGINAL PAGE IS POOR

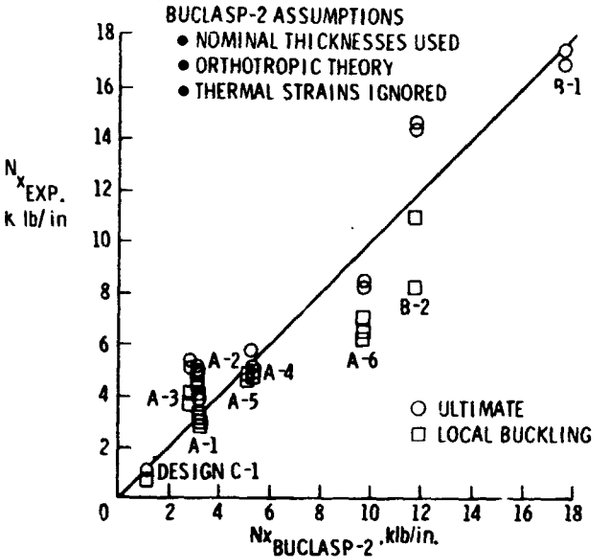

Figure 13. Comparison between analytical and experimental buckling results for local buckling specimens.

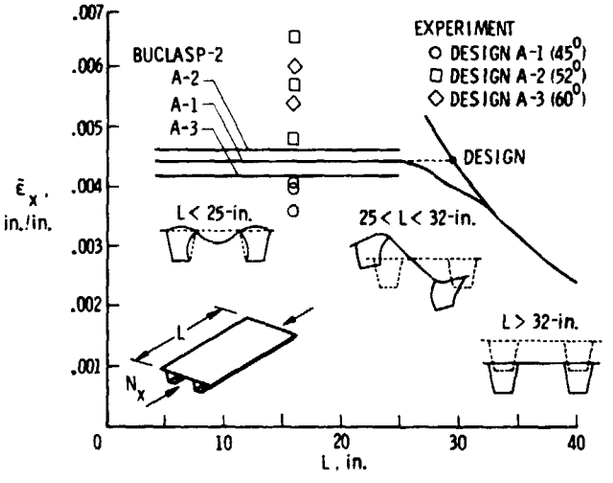

Figure 14. Buckling strain as a function of panel length for designs A-1, A-2, and A-3.

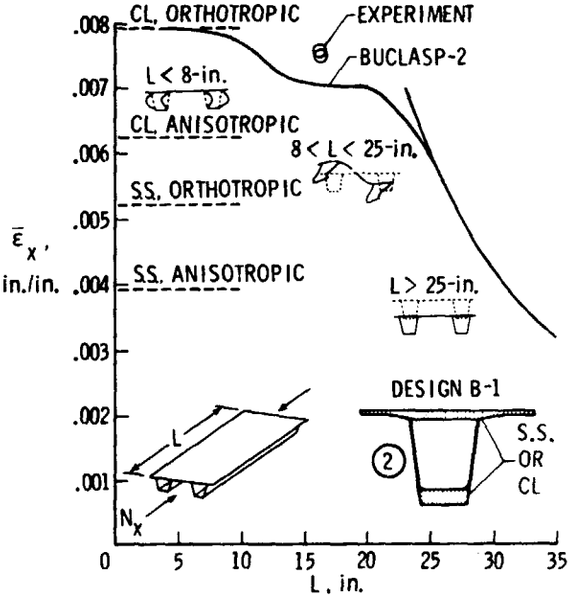

Figure 15. Buckling strain as a function of the panel length for design B-1.

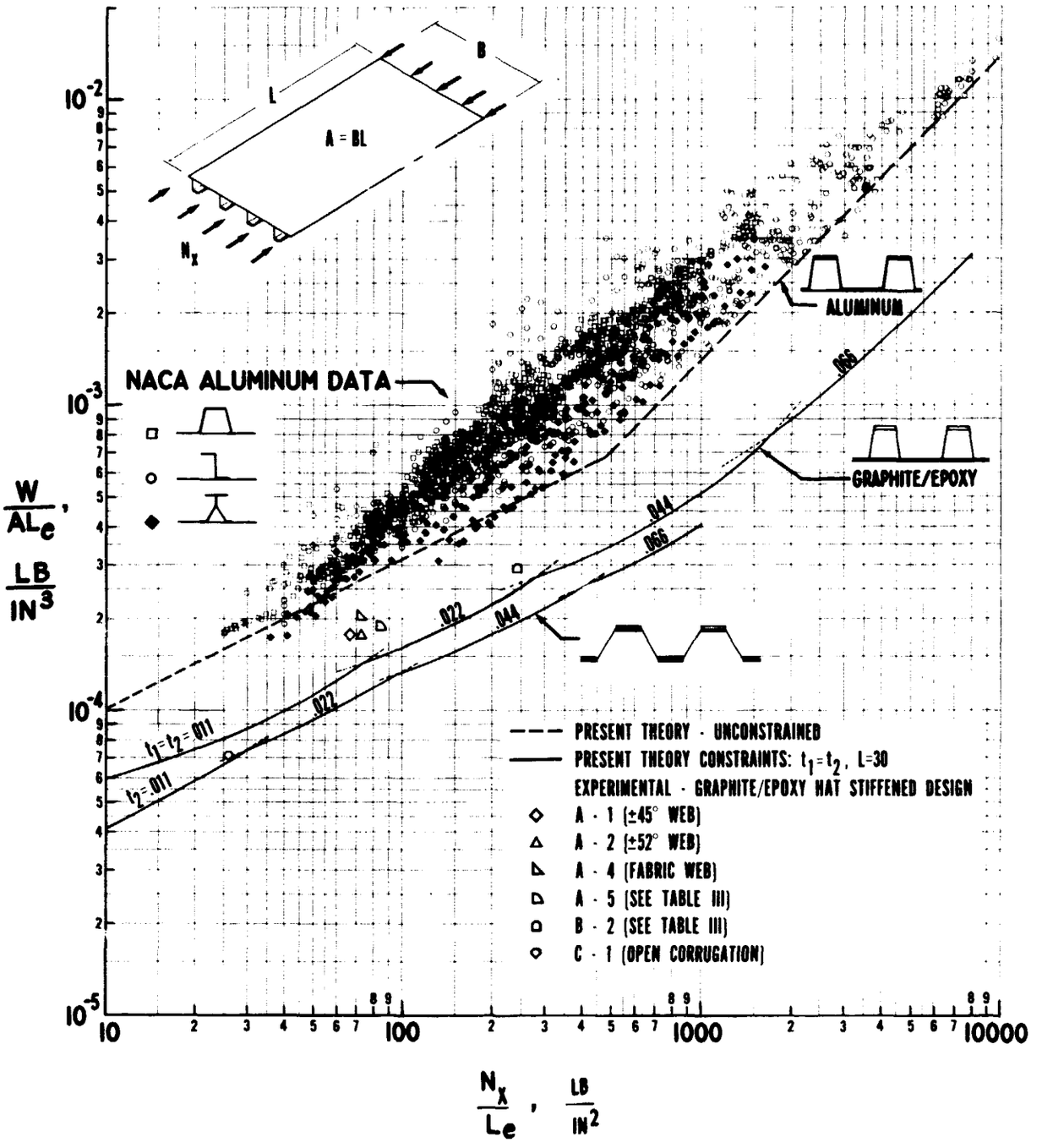

Figure 16. Comparison of structural efficiencies of graphite/epoxy and aluminum compression panels.

REPRODUCIBILITY OF THE
ORIGINAL PAGE IS POOR

Figure 17. Graphite/epoxy hat-stiffened compression panel.

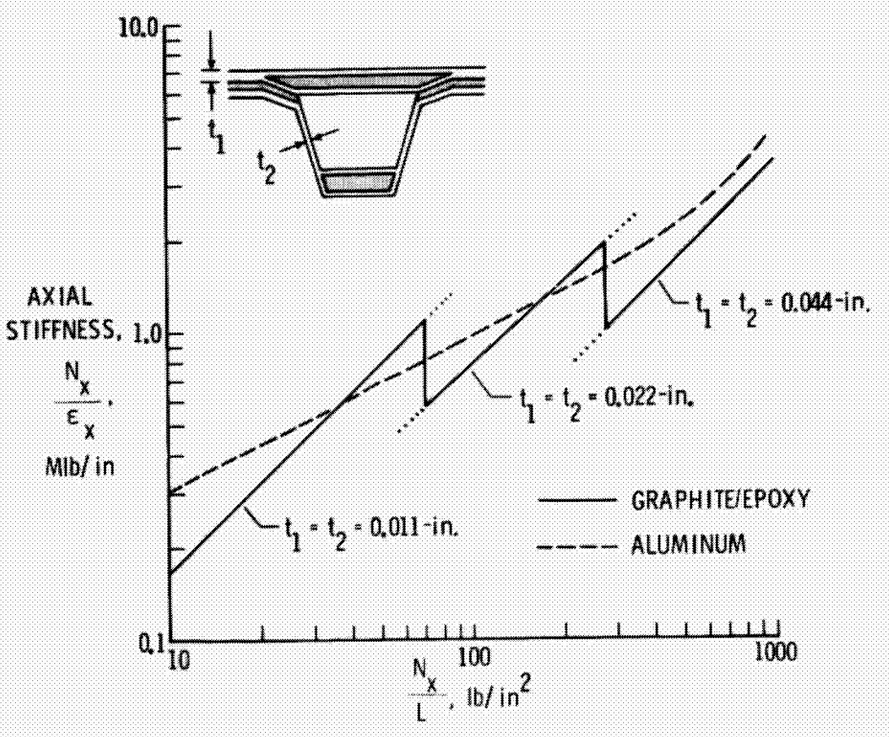

Figure 18. Comparison of axial stiffnesses of minimum weight graphite/epoxy and aluminum hat-stiffened compression panels of Figure 16.